Environmental Science and Pollution Research (2019) 26:10398–10413
https://doi.org/10.1007/s11356-019-04478-7

RESEARCH ARTICLE

Organo-modification of montmorillonite for enhancing the adsorption efficiency of cobalt radionuclides from aqueous solutions

Mohamed A. Soliman[1] · Ghada M. Rashad[2] · Mamdoh R. Mahmoud[2]

Received: 11 October 2018 / Accepted: 4 February 2019 / Published online: 14 February 2019

Abstract

Montmorillonite clay was organically modified with thoron (TH) and was employed as an adsorbent for removal of cobalt(II) radionuclides from aqueous solutions. Batch adsorption experiments, under several operational parameters such as pH, contact time, initial adsorbate concentration, adsorbent dosage, ionic strength, and temperature, were conducted to determine the optimum conditions for efficient removal of cobalt(II) radionuclides. The obtained data showed that almost complete removals were achieved for cobalt(II) at pH values ≥ 3.5 using TH-modified montmorillonite (TMM), while only 63% were obtained by unmodified clay at pH ≥ 5.4. Adsorption kinetic data of cobalt(II) were better fitted by the pseudo-second order kinetic model and its adsorption rate was controlled by film diffusion. Both Langmuir and Freundlich models had the ability to well describe the equilibrium data of cobalt(II) radionuclides at the studied temperatures. The adsorption capacity of TMM (0.85 mmol/g) was found to be not only nine times that of unmodified montmorillonite (0.097 mmol/g), but also higher than those reported in literature using various unmodified and modified clays. Thermodynamic parameters (ΔH°, ΔS°, and ΔG°) were calculated. Among the examined desorbing agents, both Al^{3+} and EDTA were succeeded to desorb most of cobalt(II) radionuclides (desorption % ~ 90%) loaded onto TMM. The results of this study clarified that TMM can be considered as an effective adsorbent for removal of cobalt(II) radionuclides from aqueous solutions.

Keywords Montmorillonite · Thoron · Cobalt · Radionuclide · Organo-clay · Adsorption

Introduction

The existence of radionuclides in radioactive liquid wastes is considered a major concern in nuclear industries. Among them, cobalt(II) radionuclide (Co-60) is an important one where it has a comparatively long half-life ($t_{1/2}$ = 5.27 years) and hard gamma radiation ($E\gamma$ = 1173.2 and 1332.5 keV). Cobalt(II) radionuclides are generated in radioactive liquid wastes by the activation of the non-radioactive cobalt(II) present in the corrosion products of reactors originating from various metal surfaces and alloys such as stellite (Abdul Nishad et al. 2012; IAEA 1981). Furthermore, irradiation of the non-radioactive cobalt(II) in research reactors and the subsequent studies at radiochemistry research laboratories also participated in the generation of cobalt(II) radionuclides in radioactive liquid wastes. From the environmental and health points of view, it is therefore mandatory to remove these radionuclides from such wastes prior their discharge into the environment.

Chemical precipitation, foam separation, solvent extraction, membrane processes, and adsorption are the traditional treatment technologies of radioactive liquid wastes (Mahmoud and Othman 2018; Gu et al. 2018; Rashad et al. 2018; Osmanlioglu 2018; Combernoux et al. 2017). Owing to its low cost, ease of operation, flexibility, and simplicity of design in addition to reversibility, adsorption technology has been successfully employed for removal of radionuclides from aqueous solutions (Han et al. 2017; Liu et al. 2017; Mahmoud et al. 2017; Wang et al. 2017) Among the various adsorbents, clays have been extensively used for removal of different pollutants, either organic or inorganic, from aqueous solutions (Długosz and Banach 2018; Zhu et al. 2018; Marcon-Brown et al. 2018; Derakhshani and Naghizadeh 2018; Ezzat et al. 2017;

Responsible editor: Georg Steinhauser

✉ Mamdoh R. Mahmoud
mamdohrefaat@yahoo.com

[1] Egypt Second Research Reactor, Atomic Energy Authority, P.O. Box 13759, Cairo, Egypt

[2] Nuclear Chemistry Department, Hot Laboratories Center, Atomic Energy Authority, P.O. Box 13759, Cairo, Egypt

Kebabi et al. 2017; Wang et al. 2017; Ferhat et al. 2016). This is because clays are characterized by their availability, low cost, high chemical and thermal stability, and large surface area as well as high cation exchange capacity. Notwithstanding that clays are successfully employed as adsorbents for decades, it is found that they exhibit low adsorption capacity particularly toward metal ions (Zhu et al. 2018; Mahmoud et al. 2017; Rashad et al. 2016; Xiao et al. 2016; He et al. 2011). Therefore, modification and development of clays are still needed to enhance their adsorption capacity for metal ions. Reviewing literature shows that many publications concerning modification of clays, organically or inorganically, for removal of metal ions have been reported (Mukhopadhyay et al. 2017; Rathnayake et al. 2017; Metwally and Ayoub 2016; Ren et al. 2014; Hoda et al. 2009; Manohar et al. 2006; Bhattacharyya and Gupta 2006). Nevertheless, organo-modification of clays using thoron (TH) has not been yet studied.

Montmorillonite is one of the most studied clay minerals in the field of environmental remediation by adsorption technology, where it possesses sorption sites not only at its interlayer space, but also on the outer surface and edges (Shahwan et al. 2006). It is an 2:1 aluminosilicate of smectite-type layered clay that has a net permanent negative charge generated by isomorphic substitutions which is balanced by interlayer exchangeable cations (Marco-Brown et al. 2018; Wang et al. 2016). However, in our previous study (Rashad et al. 2016), it is found that montmorillonite exhibited a low adsorption capacity for cobalt(II) radionuclides which are generally the disadvantage of natural clays. Therefore, the objective of the present study is to improve the adsorption capacity of montmorillonite for cobalt(II) via its organo-modification using TH as a novel modifying agent. To attain this purpose, the influential parameters on TH loading onto montmorillonite as well as on the adsorption efficiency of cobalt(II) radionuclides by the developed material, TH-modified montmorillonite (TMM), were evaluated.

Experimental

Materials and reagents

The modifying agent, thoron (TH, $C_{16}H_{11}AsN_2Na_2O_{10}S_2$), was purchased from BDH. The material to be modified, montmorillonite, was provided by Merck. The stock solution of the adsorbate, 0.05 mol/L cobalt(II), was prepared by dissolving cobalt chloride hexahydrate ($CoCl_2.6H_2O$, Fluka) in acidified distilled water. Similarly, cobalt-60 radionuclide obtained by irradiation of cobalt chloride hexahydrate in the Egypt Second Research Reactor was prepared and was used as a radiotracer during conducting the adsorption experiments of the present work. The effect of ionic strength on the present adsorption process was studied using sodium chloride (NaCl) obtained from Chem-Lab. While the inorganic reagents, calcium chloride dehydrate ($CaCl_2.2H_2O$, Panreac) and aluminum chloride hexahydrate ($AlCl_3.6H_2O$, Riedel-de-Haen), and the organic one, ethylenediaminetetraacetic acid (EDTA, Riedel-de-Haen), together with hydrochloric acid (HCl, Sigma-Aldrich) were used for desorption experiments of Co(II)-loaded adsorbent.

Synthesis of TH-modified montmorillonite

TH-modified montmorillonite was synthesized by dispersing, in 100-mL glass bottles, 10 g montmorillonite in 50 mL thoron solution of different concentrations (0–10 mmol/L) at various pH values (pH = 5.5, 7.5, and 10.3). The suspensions were kept under moderate stirring of 120 rpm at room temperature for 24 h using a magnetic stirrer. The bottles were then left to allow settling of the solid phases which were afterwards separated by decantation of the liquid phases. Samples from the liquid phases were taken off for measurement of the remaining TH concentration. The solid phases were repeatedly washed with distilled water to get rid of unadsorbed thoron, separated by decantation and eventually dried at 70 °C for 24 h. The resultant materials, TH-modified montmorillonite (abbreviated as TMM), were ground into fine particles and the 55-μm fractions obtained by sieving were stored in dark glass bottles for subsequent use.

Characterization

For qualitative analysis of the surface functional groups of the adsorbate as well as to ensure the organo-modification process of montmorillonite, the unmodified montmorillonite, the modifying agent (TH), and TMM were characterized by Fourier transform infrared spectroscopy (FTIR) using a Nicolet is 10 spectrometer (USA) in the range 4000–400 cm^{-1} with 4 cm^{-1} resolution using the KBr method. While to get as insight about the interaction of TH with montmorillonite, the X-ray diffraction patterns of the unmodified montmorillonite and the organo-modified one were compared which were recorded using a Philips PW1830 diffractometer with Cu Kα as the incident radiation.

Adsorption experiments

Adsorption experiments of cobalt(II) radionuclides onto TMM were conducted by batch technique using 5 mL adsorbate solution in 25-mL glass bottles using a thermostated water bath shaker (Karl Kolb type, D-6072, Dreieich, Germany). The effect of TH concentration (0–10 mmol/L), during synthesis of TH-modified montmorillonite at pH 5.5 (TMM-1), 7.5 (TMM-2), and 10.3 (TMM-3), on the adsorption efficiency of 0.1 mmol/L cobalt(II) spiked with cobalt-60, was studied by contacting 5 mL adsorbate solution with 0.05 g adsorbent

for 24 h at 30 °C. The influence of the solution pH was studied in the range of 2.6–7, which adjusted using a HANNA pH-meter (model HI 8519, Italy), by adding negligible amounts of HCl or NaOH to the glass bottles containing a mixture of 0.05 g adsorbent and 5 mL of 0.1 mmol/L cobalt(II) solution. The bottles were shaken at 220 rpm for 20 h at a temperature of 30 °C. The effect of TMM dosage, in the range 2–50 g/L, on the removal efficiency of the concerned radionuclide was studied by contacting the weighed solid phase with cobalt(II) solution (0.1 mmol/L) adjusted to pH 4.2 for 60 min which was more sufficient for equilibration than required. Adsorption kinetics of different initial cobalt(II) concentrations (0.1, 0.2, and 0.4 mmol/L) were investigated using contact times ranging from 1 to 120 min at a constant pH, TMM dosage, and temperature of 4.2, 0.05 g/5 mL, and 30 °C, respectively. At predetermined time intervals, the contents of the bottles were centrifuged for determination the radioactivity of cobalt(II) radionuclides in the liquid phase. The impact of ionic strength, between 0.0001 and 0.1 mol/L, adjusted using NaCl on the adsorption efficiency of 0.1 mmol/L cobalt(II) radionuclides onto 0.05 g TMM/5 mL solution, was studied at pH 4.2 by shaking this suspension for 60 min at 30 °C. Adsorption isotherms of the studied radionuclide onto 0.05 g TMM/5 mL solution were performed using different initial adsorbate concentrations in the range 0.4–7 mmol/L at various temperatures of 30, 45, and 60 °C. The solution pH was kept constant at 4.2, while the contact time was set at 60 min.

Prior analysis process, the solid phase was separated by centrifugation using a Chirana centrifuge at 4500 rpm for 5 min. Thoron concentration in supernatant of the collected samples during synthesis of TMM was determined spectrophotometrically using a Spectronic-20 UV-Vis spectrophotometer. Whereas, the radioactivity of cobalt(II) radionuclides before and after the adsorption process onto TMM was measured radiometrically using a single-channel gamma-radiation spectrometer (Spectech ST360, USA). Based on these measurements, the amount of adsorbate, either TH or cobalt(II), adsorbed (Q, mmol/g) was calculated using the following relation:

$$Q = \left[\frac{\text{removal}\ (\%)}{100}\right] \times C_{\mathrm{o}} \times \left[\frac{V}{M}\right] \quad (1)$$

where C_{o} is the initial concentration of adsorbate (mmol/L), V is the volume of solution (L), and M is the weight of the adsorbent (g). The removal percentage in the above equation was calculated as follows:

$$\text{Removal}\ (\%) = \left[\frac{A_{\mathrm{i}} - A_{\mathrm{f}}}{A_{\mathrm{i}}}\right] \times 100 \quad (2)$$

where A_{i} and A_{f} are the initial and final radioactivity of Co(II) radionuclides in the liquid phase, respectively.

Desorption study

Prior to desorption experiments, the organo-modified montmorillonite (0.1 g) was contacted with 5 mL of 0.2 mmol/L cobalt(II) ion, spiked with cobalt-60, at pH ~ 4.2 for 60 min. The cobalt(II)-loaded TMM, separated by centrifugation, was dispersed into 5 mL of the desorbing agent and aged under stirring at 120 rpm for 24 h. After centrifugation and measuring the radioactivity of cobalt(II) radionuclides in the supernatant, the desorption percentage of the concerned radionuclide was calculated using the relation:

$$\text{Desorption}\ (\%) = \frac{\text{desorbed amount of cobalt(II)}}{\text{adsorbed amount of cobalt(II)}} \times 100 \quad (3)$$

Results and discussion

Characterization

The FTIR spectra of montmorillonite, TH, and TMM are represented in Fig. 1 a. The absorption bands at 3631 cm^{-1}, 3446 cm^{-1}, 1635 cm^{-1}, 1047 cm^{-1}, 917 cm^{-1}, 815 cm^{-1}, 528 cm^{-1}, and 463 cm^{-1} observed in the spectra of montmorillonite and the modified one are characteristics of montmorillonite clay. The absorption band at 3631 cm^{-1} is assigned to the stretching vibration of octahedral OH groups (Al–OH and Mg–OH). The OH stretching vibration of the interlayer water is observed by the broad absorption band centered at 3446 cm^{-1}, while its bending vibration is appeared at 1635 cm^{-1}. The strong absorption band at around 1047 cm^{-1} with a shoulder at 917 cm^{-1} is ascribed to the stretching vibration of Si–O–Si. The bands at 815 cm^{-1} and 528 cm^{-1} are attributed to the bending vibrations of Si–O–Al and Si–O–Mg, respectively. The bending vibration of Si–O–Si is observed at 463 cm^{-1}. The additional absorption bands at 1511 cm^{-1} and 1383 cm^{-1} for TMM are characteristics for C–C and C–N ring stretching vibrations. These bands together with that found at 1186 cm^{-1} (due to S=O stretching vibration of sulfonate groups of TH) are an evidence for loading of TH onto montmorillonite and hence the success of the modification process.

In order to acquire some information about the binding mode of TH with montmorillonite, either at the clay surface or at the interlayer region, the concerned clay was further characterized by XRD before and after the organo-modification process. Figure 1 b compares the XRD pattern of unmodified montmorillonite with that of TMM. This figure shows that montmorillonite and TMM have a basal d spacing (d_{001}) of 12.26 and 12.29 A°, respectively. This insignificant change in the d spacing suggested that TH bound with montmorillonite at its surface rather than at the interlayer space.

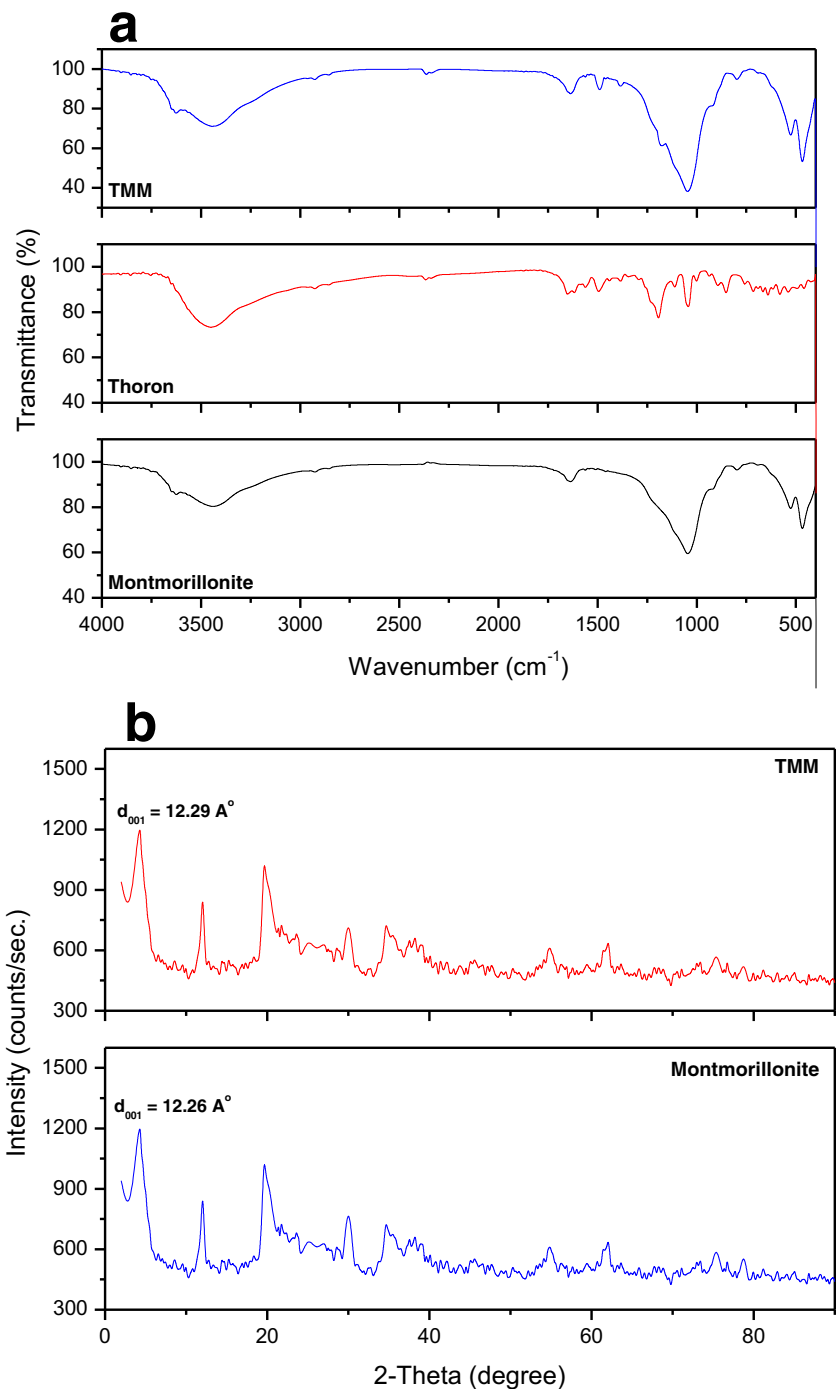

Fig. 1 FTIR spectra of montmorillonite, thoron, and TMM (**a**) and XRD patterns of montmorillonite and TMM (**b**)

Effect of TH concentration

The effect of TH concentration on its adsorption capacity onto montmorillonite as well as the adsorption efficiency of cobalt(II) radionuclides onto the modified clay is illustrated in Fig. 2. The relation between the concentration of TH and its amount adsorbed onto montmorillonite at various pH values (pH = 5.5, 7.5, and 10.3) is shown in Fig. 2 a. This figure indicates that the amount of TH adsorbed by montmorillonite is obviously dependent on its initial concentration and the solution pH. Expectedly, increasing TH concentration resulted in an increase in the adsorption capacity of this modifying agent (Fig. 2a). On the other hand, the amount of TH adsorbed onto the concerned clay is decreased with increasing the pH of the solution particularly at initial TH concentrations ≥ 1 mmol/L. This reduction can be attributed to (i) the competition between TH molecules and OH^- ions for

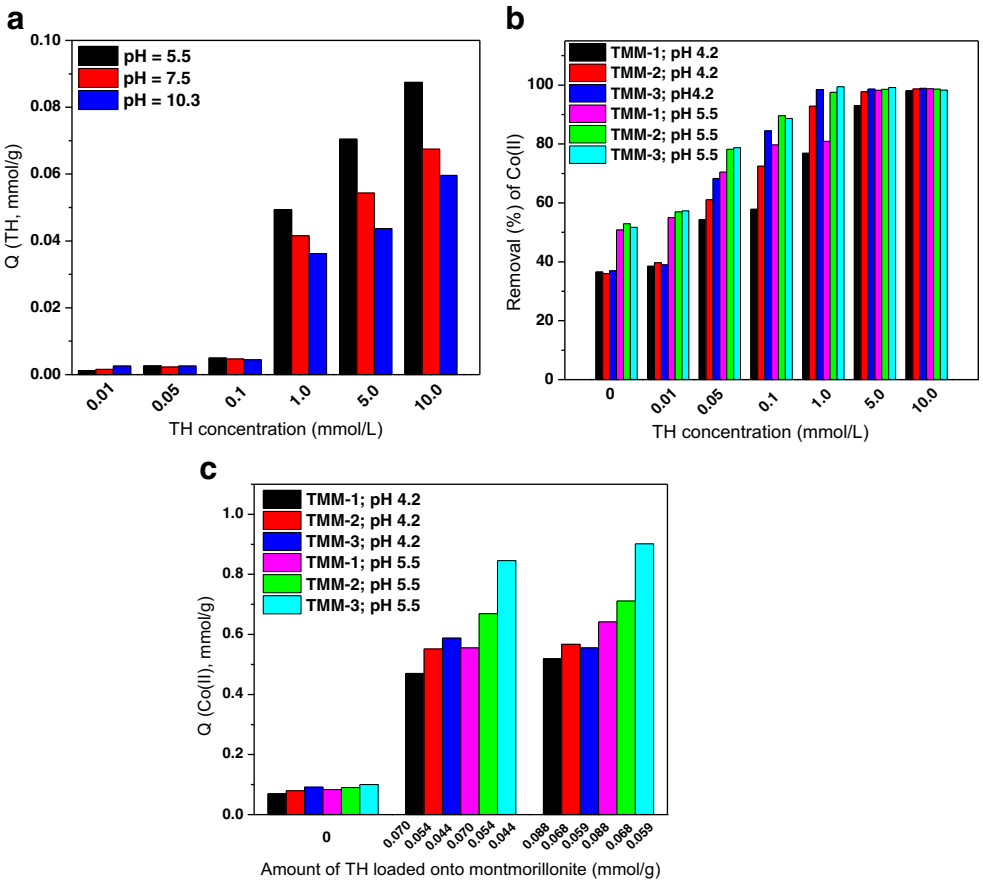

Fig. 2 Effect of TH concentration on its adsorption capacity onto montmorillonite (**a**) and the adsorption efficiency of cobalt(II) radionuclides onto the modified clay (**b** and **c**)

adsorption onto montmorillonite and (ii) decreasing the binding sites available onto montmorillonite due to increasing the number of dissociated functional groups with increasing the solution pH.

The influence of TH concentration (0–10 mmol/L), during synthesis of TH-modified montmorillonite at pH 5.5, 7.5, and 10.3 which respectively denoted as TMM-1, TMM-2, and TMM-3, on the removal percentage of cobalt(II) radionuclides is studied at pH 4.2 and 5.5, and the obtained results are shown in Fig. 2 b. As evident by this figure, the removal percentage of cobalt(II) radionuclides is affected by the loading pH of TH as well as that of cobalt(II) solution particularly at TH concentration range of 0.05–1 mmol/L. The data depicted in Fig. 2 b reveal that it was difficult to determine the optimum conditions for TH loading onto montmorillonite that required for efficient removal of cobalt radionuclides. Therefore, the adsorption capacity of cobalt(II) using TH-modified montmorillonite, synthesized at different pH values, was experimentally determined and compared with that of the unmodified one (Fig. 2c). From this figure, it can be seen that the adsorption capacity of cobalt(II) is slightly affected by the loading pH of TH, while significantly influenced by the solution pH of the adsorbate. This figure also shows that maximum adsorption capacity of 0.85 mmol/g is achieved for cobalt using TMM synthesized at pH 10.3, TMM-3, which is nearly nine times higher than that of unmodified montmorillonite (0.097 mmol/g). Since there is no considerable variation between values of the adsorption capacity of cobalt at 5 and 10 mmol/L, there was no need to use the higher concentration of TH for modifying montmorillonite. Based on the data given in Fig. 2 c, the subsequent adsorption experiments of cobalt(II) was carried out using TMM synthesized at pH 10.3 (TMM-3) using 5 mmol/L TH.

Effect of the solution pH

Figure 3 represents the effect of the initial pH of the solution, pH_i, on the removal efficiency of cobalt(II) radionuclides by adsorption technology, using unmodified montmorillonite and the organo-modified one (TMM), and the precipitation method. Besides, the relation between the initial pH of the solution and the final one, pH_f, for the previously mentioned two adsorbents, is also depicted in this figure. By using montmorillonite as an adsorbent, the data presented in Fig. 3 reveal that the removal percentage of cobalt(II) radionuclides is gradually increased with increasing the initial pH of the solution and reached its ultimate value of about 63% at the initial pH range 4.9–6.3. Further increase in the pH_i value resulted in a slight increase in the removal percentage of cobalt(II) radionuclides. While the utilization of organo-modified montmorillonite,

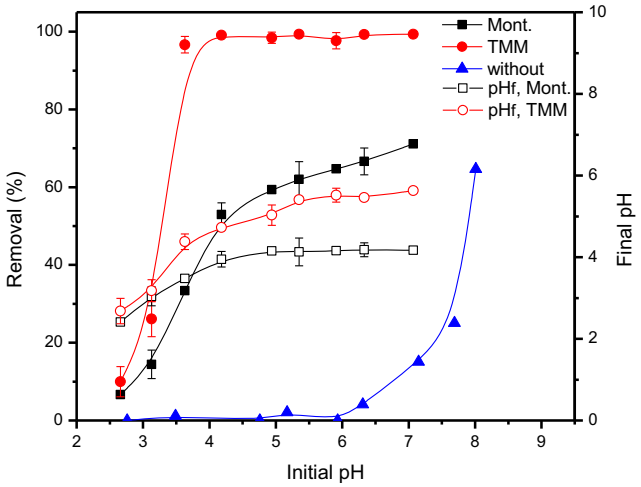

Fig. 3 Effect of the initial pH of the solution on the removal percentage of cobalt(II) radionuclides using montmorillonite and TMM

TMM is not only improved the removal percentage of cobalt(II) radionuclides, but also increased the pH range of the ultimate removal and extended it to more acidic values. The removal percentage of cobalt(II) using TMM is abruptly increased with increasing the solution pH_i where about 10% and 96% of the studied radionuclide are removed at pH_i values of 2.6 and 3.6, respectively. Obviously, almost complete removals for cobalt(II) are achieved in the pH_i range 3.6–7.1 using TMM. During the inspection of the chemical structure of the modifying agent, thoron(TH), it is found that it has five functional groups. The dissociation constants of the sulfonate groups are corresponding to pK_1 and pK_2 values < 1.3. The two arsono groups have dissociation constants corresponding to pK_3 and pK_4 values of 3.7 and 8.3, while the phenolic group has a dissociation constant corresponding to pK_5 value of 11.8 (Margerum et al. 1953). This means that the current modification process using this modifying agent provided the montmorillonite's surface with variant adsorption sites. Accordingly, the efficient removals obtained for cobalt(II) radionuclides at relatively low pH values, $pH_i < 4.5$, using the modified montmorillonite can be attributed mainly to the occurrence of sulfonate groups ($–SO_3H$, which dissociated at a low pH value) at montmorillonite's surface. At lower pH values, the competition between H^+ and cobalt(II) cations for adsorption onto TMM may be responsible for the reduction in the removal efficiency. The effectiveness of TMM for adsorption of cobalt(II) radionuclides over the studied pH_i range, when compared to the unmodified montmorillonite, is attributed to the presence of higher number of adsorption sites due to the modification process.

The relation between the pH_i and pH_f (Fig. 3) indicates that TMM and the unmodified montmorillonite exhibit buffering capacities in the initial pH range 4–7. However, the variation in the pH_f values between the unmodified montmorillonite and TMM may be owing to the change in the surface properties of montmorillonite due to binding of the modifying agent, TH, which could affect the acid-base interactions at the adsorbent surface. This is because such binding may obscure many functional groups, mainly –OH groups, at montmorillonite's surface and hence clogged their contribution to the acid-base interactions. Regarding the data obtained for cobalt(II) radionuclide by the precipitation method (Fig. 3), it can be observed that no removals are recorded at pH_i values below 6, whereas higher pH_i values increased the removal efficiency which reached to about 65% at pH 8. This implies that the removals observed at $pH \leq 6$ for cobalt(II) radionuclides by using montmorillonite and TMM are primarily due to adsorption, while those at pH_i values more than 6 may be owing to the combination of adsorption and precipitation processes. Consequently, adsorption experiments of cobalt(II) radionuclides onto the modified montmorillonite were performed at a pH_i value below 6, specifically 4.2, to avoid its removal by precipitation.

Effect of TMM content

From the economic and waste management points of view, it is substantial to determine the most appropriate amount of an adsorbent required for an adsorption system. Therefore, the effect of the TMM dosage (2–50 g/L ≡ *V/M* in the range 0.5–0.02 L/g) on the adsorption efficiency of cobalt(II) radionuclides is investigated at pH 4.2 and the results obtained are shown in Fig. 4. This figure demonstrates that both the removal percentage and the adsorbed amount of cobalt(II) radionuclides are significantly influenced by the dosage of the modified montmorillonite. Increasing the TMM dosage from 2 g/L (*V/M* = 0.5) to 20 g/L (*V/M* = 0.05) increased the removal percentage from 21.5 to 99.2%, whereas decreased the adsorbed amount from 0.199 to 0.084 mmol/g. Further increase in the TMM content had no effect on the removal percentage of

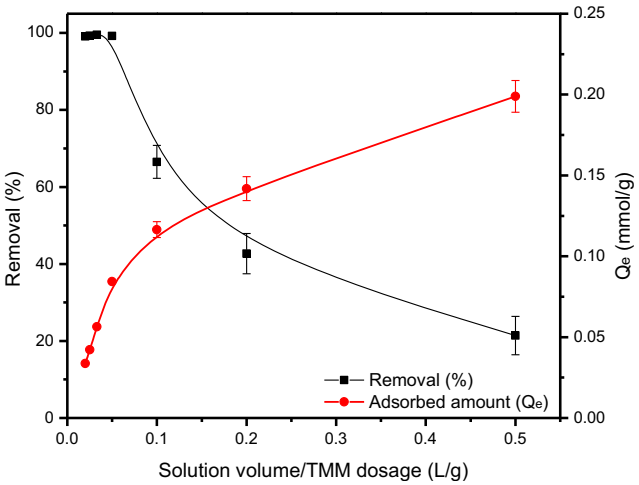

Fig. 4 Effect of the TMM dosage on the removal percentage and the adsorbed amount of cobalt(II) radionuclides

cobalt(II) radionuclides while markedly reduced its adsorbed amount. Enhancement in the removal percentage of cobalt(II) radionuclides with increasing the solid-phase content is attributed to the increase in the number of functional groups, required for the adsorption process, at the modified montmorillonite surface. Increasing the removal efficiency with increasing the solid content has been previously reported for many adsorption systems (Mahmoud et al. 2017; Rashad et al. 2016; Chen et al. 2012; Guo et al. 2011). On the other hand, higher adsorbent dosages increase the eventuality of collisions between TMM particles and hence create particle aggregation. Thus, the total surface area of the solid phase decreased while the diffusion path length increased, which conduce to the decrease in the adsorption capacity observed in Fig. 4 for cobalt(II) radionuclides (Chen et al. 2012). Additionally, the reduction in the adsorbed amount of cobalt(II) radionuclides with increasing the content of TMM can also be mathematically explained as follow. During calculation of the adsorbed amount of cobalt(II) at different dosages of TMM based on Eq. 1, the denominator (M) increased largely which giving rise to a decrease in the quotient. Although R% at the numerator is increased with increasing the TMM dosage, but this increase is low compared to the content of the adsorbent. At $V/M \geq 0.1$ L/g ($M = 20$ g/L), almost complete removals of cobalt(II) radionuclides are attained, thereby M became the only exchangeable parameter in the above relation and its increase resulted in further decrease in the value of the adsorbed amount. Referring to our previous study (Rashad et al. 2016), it is found that unsatisfactory removal efficiency (R% ~ 70%) is obtained for cobalt(II) radionuclides using montmorillonite even at a relatively high adsorbent dosage (100 g/L). Comparing those data with the results of the present study reflects the importance of the modification process where almost complete removals are achieved using only 20 g/L organo-montmorillonite.

Kinetic studies

Effect of contact time

It is well recognized that contact time is one of the most important parameters for evaluating the performance of an adsorption process. Therefore, the effect of contact time on the removal percentage of 0.1, 0.2, and 0.4 mmol/L cobalt(II) radionuclides using TMM (0.05 g/5 mL adsorbate solution) is presented in Fig. 5. Before reaching equilibrium, the data given in this figure show that adsorption process of cobalt(II) radionuclides onto the modified montmorillonite is governed by two steps. In the first step, the removal percentage of cobalt(II) is sharply increased with increasing time and most of cobalt(II) ions (~ 92%, 55%, and 28% for 0.1, 0.2, and 0.4 mmol/L, respectively) are uptake within 5 min. This adsorption behavior is attributed to the availability of numerous

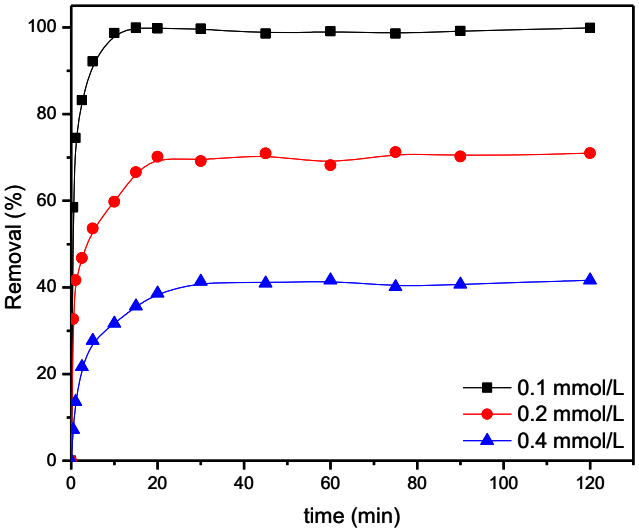

Fig. 5 Effect of contact time on adsorption efficiency of different initial concentrations cobalt(II) radionuclides by TMM

adsorption sites onto the surface of TMM. In the second step, the increase in the removal percentage of cobalt(II) is relatively slow, which may be due to hindrance of adsorption of further ions caused by those previously adsorbed in the first step. This hindrance resulted in a decrease in the adsorption rate of cobalt(II) radionuclides in the second step (Yao et al. 2017). The data represented by Fig. 5 also reveal that the removal percentage achieved at equilibrium and the equilibrium time of the present adsorption process is obviously dependent on the initial adsorbate concentration. Maximum removal percentages of 41.2%, 69.9%, and 99.7% are achieved for initial cobalt(II) concentrations of 0.4 mmol/L, 0.2 mmol/L, and 0.1 mmol/L at equilibrium times of 30 min, 20 min, and 10 min, respectively. In order to ensure equilibration, contact time of 60 min was chosen for the subsequent adsorption experiments. In general, it is reported that retention of adsorbates by 2:1 clay minerals which contain both internal and external adsorption sites is a slow process (Sparks 2003). In the current investigation, cobalt(II) radionuclides are rapidly adsorbed onto the modified montmorillonite, an 2:1 clay mineral. This finding suggested that adsorption of cobalt(II) ions is mostly took place by the active sites of the modifying agent, thoron that externally adsorbed onto montmorillonite's surface, rather than the internal adsorption sites of montmorillonite.

Modeling of kinetic data

For designing of an adsorption system, it is important to predict the adsorption rate of an adsorbate onto an adsorbent. For this purpose, the adsorption kinetic data of cobalt(II) radionuclides onto TMM are analyzed by four frequently used adsorption kinetic models. These models are Lagergren pseudo-first order, pseudo-second order, Ritchie second-order, and Elovich.

The Lagergren kinetic model states that the adsorption rate of a species onto a solid phase is proportional to the number of unoccupied sites and it is followed a pseudo-first order equation (Lagergren 1898). The linear form of this model is expressed as follows:

$$\log(Q_e - Q_t) = \log Q_e - \left(\frac{K_1}{2.303}\right)t \quad (4)$$

where Q_e and Q_t are the amount of cobalt(II) adsorbed (mmol/g) at equilibrium and at time t, respectively, while K_1 is the rate constant of the pseudo-first order adsorption process (min^{-1}). A straight line of log ($Q_e - Q_t$) versus t proposes the applicability of this model. The intercept and the slope of the plot are used to determine the values of Q_e and K_1, respectively.

Proportional of the adsorption rate of an adsorbate to the square number of unoccupied sites of an adsorbent is the assumption of the pseudo-second order kinetic model (Ho and McKay 1999). The linearized form of this model is represented as follows:

$$\frac{t}{Q_t} = \frac{1}{K_2 Q_e^2} + \left(\frac{1}{Q_e}\right)t \quad (5)$$

where K_2 is the rate constant of the pseudo-second order kinetic model (g/mmol min). For applicability of this model, the plot of t/Q_t against t should give a straight line from which Q_e and K_2 can be calculated from the slope and intercept, respectively.

The Ritchie second-order kinetic model is usually used to measure the initial particle loading, which is linearly expressed by the following equation (Mahmoud et al. 2015):

$$\left[\left(\frac{Q_e}{Q_e - Q_t}\right) - 1\right] = K_3 t \quad (6)$$

where K_3 is the Ritchie second-order rate constant of adsorption (min^{-1}) which can be estimated from the slope of the linear plot of ($[Q_e/(Q_e - Q_t)] - 1$) versus t.

The Elovich kinetic model is used to describe the kinetics of chemisorption on energetically heterogeneous solid surface and it is based on the assumption that the adsorption sites increase exponentially with adsorption, which implies a multilayer adsorption (Mahmoud et al. 2014). The linear form of this model is given by the following relation:

$$Q_t = \frac{1}{\beta}\ln(\alpha\beta) + \left(\frac{1}{\beta}\right)\ln t \quad (7)$$

where α is the initial adsorption rate (mmol/g min) and β is a parameter related to the extent of surface coverage and activation energy for chemisorption. The values of α and β are estimated from the intercept and slope of the linear plot of Q_t versus ln t.

Linear fittings of the kinetic data of the present adsorption process, at the studied initial cobalt(II) concentrations, to the abovementioned four kinetic models are shown in Fig. 6. The calculated kinetic parameters together with the correlation coefficients (R^2) of the plots are also represented in this figure (Table 1). Regarding the linear plots and the correlation coefficient values of the applied kinetic models, it can be noted that satisfactory R^2 values are obtained which implies that the four kinetic models used in the present study had the ability to well represent the current adsorption process. Nevertheless, throwing more light on the R^2 values of the studied kinetic models (Fig. 6; Tables 1), it can be observed that the pseudo-second order kinetic model exhibited the highest values (R^2 = 0.999) at all the studied cobalt(II) concentrations. Based on this observation, it is concluded that the adsorption kinetics of cobalt(II) radionuclides onto TMM are better described by the pseudo-second order kinetic model. Additionally, the kinetic parameters of the pseudo-second order kinetic model (Fig. 6b; Table 1) indicate that the calculated amount of Co(II) adsorbed per gram of TMM, Q_e (mmol/g), increased with increasing the initial adsorbate concentration, while the values of the adsorption rate, K_2 (g/mmol min), decreased with increasing the initial cobalt(II) concentration. Increasing the K_2 value with decreasing the initial adsorbate concentration suggested that the rate of cobalt(II) adsorption onto TMM increased with decreasing the initial adsorbate concentration and hence equilibrium is attained much faster, which is in a good agreement with the experimental data.

Furthermore, the time-dependent adsorption data are analyzed by two commonly used kinetic models, namely, intraparticle and film diffusion models, in order to identify the diffusion mechanism of the present adsorption process. The linear form of the intraparticle diffusion model suggested by Weber and Morris is expressed by the following equation (Weber and Morris 1963):

$$Q_t = K_4 t^{0.5} + C \quad (8)$$

where K_4 is the intraparticle diffusion constant (mmol/g $min^{0.5}$) and C is the intercept (mmol/g). If the intraparticle diffusion is the rate-controlling step for an adsorption process, the plot of Q_t versus $t^{0.5}$ should give a straight line passing through the origin. On the other hand, the film diffusion model suggested by Boyd is represented as follow (Boyd et al. 1947):

$$F = 1 - \left(\frac{6}{\pi^2}\right)\exp(-Bt) \quad (9)$$

where Bt is a mathematical function of F, and F is the fraction of adsorbate adsorbed at different time t, which is given by:

$$F = \frac{Q_t}{Q_e} \quad (10)$$

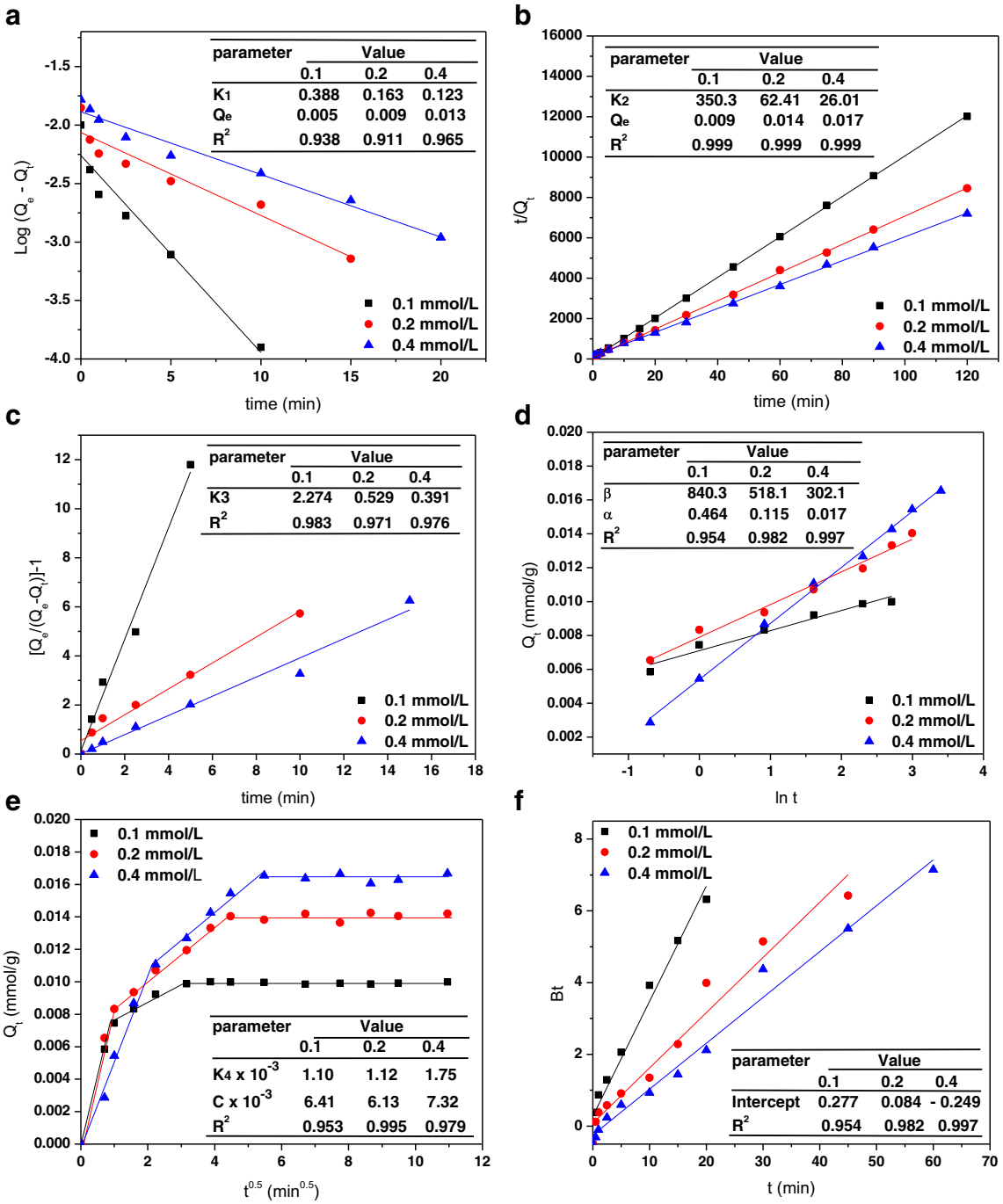

Fig. 6 Linear fittings of the kinetic data of cobalt(II) radionuclides onto TMM to pseudo-first order (**a**), pseudo-second order (**b**), Ritchie second order (**c**), Elovich (**d**), intraparticle diffusion (**e**), and Boyd (**f**) kinetic models

Substituting Eq. (10) into Eq. (9), the kinetic expression becomes:

$$Bt = -0.4977 - \ln\left(1 - \frac{Q_t}{Q_e}\right) \quad (11)$$

For a particle diffusion mechanism of an adsorption process, the plot of Bt versus t should result in a straight line with zero intercept. If not, the adsorption process is governed by film diffusion. Linear fittings of the experimental adsorption kinetic data of cobalt(II) radionuclides onto TMM to Weber and Morris (Eq. 8) and Boyd (Eq. 11) diffusion models are shown in Fig. 6 e and f, respectively. At all the studied initial cobalt(II) concentrations, the plots of Q_t versus $t^{0.5}$ did not yield straight lines passing through the origin. Instead, Weber-Morris plots show multi-linearity. The first and the second portions can be attributed to external surface

Table 1 Comparison of the adsorption capacity of TH-modified montmorillonite with those reported in literature for metal ions using natural, organo-modified, and inorgano-modified clays

Adsorbent	Adsorbate	Q_{max} (mg/g)	Reference
Kaolinite Montmorillonite	Vanadium(V)	0.78 0.98	Zhu et al. 2018
Bentonite	Uranium(VI)	9.124	Wang et al. 2017
Attapulgite	Uranium(VI)	9.35	Han et al. 2017
Vermiculite H_2O_2 sonicated vermiculite	Manganese(II)	28.32 36.77	Kebabi et al. 2017
Polyaniline-bentonite	Uranium(VI)	17.5	Liu et al. 2017
Ti-pillard smectite	Arsenic(III)	0.157	Mukhopadhyay et al. 2017
ODTMA-montmorillonite ODTMA-Al-montmorillonite	Chromium(VI)	9.61 17.86	Rathnayake et al. 2017
Kaolinite	Lanthanum(III) Neodymium(III)	1.731 1.587	Xiao et al. 2016
	Yttrium(III)	0.971	
Bentonite	Zinc(II) Cupper(II)	21.8 23.5	Ferhat et al. 2016
Diatomite	Cobalt(II)	8.721 8.136	Rashad et al. 2016
Sepiolite bentonite		7.924	
Illite	Uranium(VI)	5.266	Gao et al. 2015
CTAB-Fe-montmorillonite	Arsenic(III) Arsenic(V)	13.89 8.85	Ren et al. 2014
Fe-montmorillonite	Arsenic(III)	16.13	
	Arsenic(V)	15.15	
Bentonite APS-bentonite	Lead(II)	20.684 27.652	Guerra et al. 2013
AEAPS-bentonite		29.541	
Fe-sepiolite	Cobalt(II)	24.326	Lazarevic et al. 2012
Diatomite Calcined diatomite	Thorium(IV)	6.961 13.924	Yusan et al. 2012
Palygorskite	Cobalt(II)	8.88	He et al. 2011
Kaolinite	Cadmium(II) Nickel(II)	0.88 0.90	Jiang et al. 2010
	Cupper(II)	1.22	
Formaldehyde-bentonite	Cobalt(II)	21.381	Omar et al. 2009
Kaolinite	Lead(II) Cadmium(II)	16.16 10.75	Unuabonah et al. 2008
Sodium tetraborate-kaolinite	Lead(II)	42.92	
	Cadmium(II)	44.05	
8HQ-immobilized bentonite	Cupper(II)	56.55	Gok et al. 2008
Al-pillard bentonite	Cobalt(II)	38.521	Manohar et al. 2006
TBA-kaolinite TBA-montmorillonite	Cupper(II)	3.2 27.3	Bhattacharyya and Gupta 2006
Montmorillonite TH-modified montmorillonite	Cobalt(II)	5.717 50.09	This work

ODTMA, octadecyltrimethylammonium; *CTAB*, cetyltrimethylammonium; *APS*, 3-aminopropyltrimetoxisilane; *AEAPS*, 3,2-aminoethylaminopropyltrimetoxisilane; *8HQ*, 8-hydroxyquinoline; *TBA*, tetrabutylammonium

adsorption (film diffusion) and intraparticle diffusion (pore diffusion) of cobalt(II) radionuclides, respectively, while the third linear portion is due to equilibrium. The slope and intercept of the second linear portion s are used to calculate values of the intraparticle diffusion constant, K_4, and C. The obtained data together with R^2 values of the second linear portions are presented in Fig. 6 e (Table 1). Based on the plots represented in this figure, the intraparticle diffusion was not the rate-

controlling step during adsorption of cobalt(II) radionuclides onto TMM. On the other hand, the results demonstrated in Fig. 6 f indicate that plots of Bt versus time resulted in straight lines with high correlation coefficients ($R^2 = 0.954$, 0.982, and 0.997 for 0.1, 0.2, and 0.4 mmol/L cobalt(II)). But, these plots had non-zero intercepts as shown by the obtained data, indicating that adsorption rate of cobalt(II) radionuclides onto the modified montmorillonite is controlled by film diffusion.

Effect of ionic strength

It is well known that ionic strength is one of the essential parameters for adsorption technology owing to its importance in participation of elucidation of the adsorption mechanism. The results of studying this parameter can be used to differentiate between outer-sphere complexation and inner-sphere complexation. In general, outer-sphere complexation is the predominant adsorption mechanism if adsorption process of an adsorbate onto an adsorbent is obviously influenced by ionic strength, whereas inner-sphere surface complexation is unaffected by ionic strength (Sparks 2003; Guo et al. 2011; Chen and Wang 2007). Thereby, adsorption process of cobalt(II) radionuclides onto the modified montmorillonite was carried out from solutions of low, moderate, and relatively high ionic strengths (0.0001–0.1 M NaCl). The results obtained are shown in Fig. 7. As shown by the data given in this figure, the removal percentage of cobalt(II) radionuclides (R% > 99%) is unaffected by increasing the background electrolyte concentration up to 0.001 M. Beyond this concentration, the removal percentage is markedly reduced and reached to about 40% at 0.1 M NaCl. The apparent dependence of the removal percentage of cobalt(II) radionuclides on ionic strength of the solution suggested that outer-sphere surface complexation is the dominant adsorption mechanism in the present investigation.

Equilibrium studies

Adsorption isotherms

Adsorption isotherm is a graph that describes the relation between the equilibrium concentration of an adsorbate and its amount adsorbed onto the solid phase at fixed temperature, pressure and solution chemistry such as pH and ionic strength (Essington 2004). Adsorption isotherms of cobalt(II) radionuclides onto the modified montmorillonite, at various temperatures of 30, 45, and 60 °C, are investigated at a constant pH value of about 4.2 and a fixed adsorbent weight of 10 g/L. The obtained equilibrium data are shown in Fig. 8. This figure demonstrates that the equilibrium adsorption capacity, Q_e, of cobalt(II) radionuclides is markedly influenced by its initial concentration and the reaction temperature. Increasing the initial cobalt(II) concentration resulted in an increase in the Q_e value, at all the studied temperatures, with adsorption isotherms shape of L type according to the Giles classification (Giles et al. 1960). This L-shaped (Langmuir) isotherm, which is the most commonly encountered type of isotherm in soil chemistry, clarifies that the solid surface has a relatively high affinity for low concentrations of the adsorbate. By increasing the adsorbate concentration, its affinity for the solid surface decreases where the surface coverage increases (Essington 2004), which is observed in the present study (Fig. 8). On the other hand, the equilibrium adsorption capacity of cobalt(II) radionuclides is unaffected by the reaction temperature at the low studied adsorbate concentrations, while it is noticeably influenced by temperature at high cobalt(II) concentrations. At the highest studied cobalt(II) concentration,

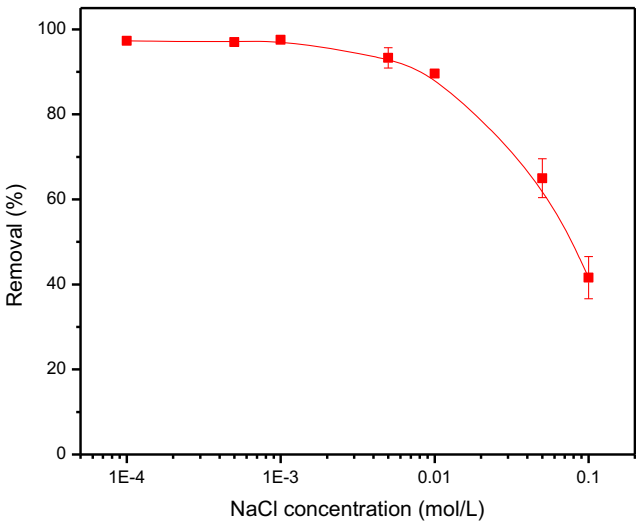

Fig. 7 Effect of ionic strength on the removal efficiency of cobalt(II) radionuclides using TMM

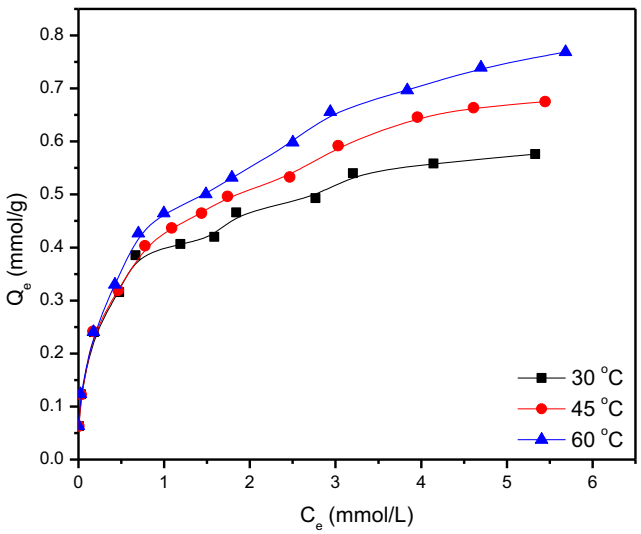

Fig. 8 Equilibrium isotherms of cobalt(II) radionuclides onto TMM at various temperatures

increasing the temperature from 30 to 60 °C increased the adsorption capacity from 0.576 to 0.769 mmol/g. This enhancement in the adsorption capacity with increasing temperature suggested that adsorption of cobalt(II) radionuclides onto TMM is an endothermic process.

Modeling of adsorption isotherms data

Generally, modeling of the equilibrium data is important to determine the appropriate isotherm models for design of an adsorption system. Four adsorption isotherm models, namely, Langmuir, Freundlich, Temkin, and generalized models, are used in the present study to analyze the adsorption isotherms data of cobalt(II) radionuclides onto TMM at the studied temperatures. The theoretically derived Langmuir equation assumes that (i) adsorption occurs on solid surfaces that have a fixed number of identical sites; (ii) monolayer coverage is permitted and equilibrium is attained; (iii) adsorption process is reversible; (iv) there is no interaction between adsorbed species; and (v) adsorption occurs on homogenous solid surfaces. Most of these assumptions are not valid for heterogeneous solid surfaces such as clays. Consequently, the Langmuir equation should only be used for purely qualitative and descriptive purposes (Sparks 2003). The linearized form of the Langmuir adsorption equation is expressed as (Langmuir 1918):

$$\frac{C_e}{Q_e} = \frac{1}{Q_m K_L} + \frac{C_e}{Q_m} \tag{12}$$

where C_e is the equilibrium concentration of cobalt(II) in the aqueous phase (mmol/L), Q_e is the amount of cobalt(II) adsorbed per gram of the solid phase at equilibrium (mmol/g), and Q_m is the maximum adsorption capacity and has the unit of Q_e. The Langmuir adsorption constant, K_L, is a measure of the intensity of adsorption (L/g). For this expression, a plot of C_e/Q_e against C_e should yield a straight line with a slope of $1/Q_m$ and a Y-intercept of $1/Q_m K_L$, if this model describes the adsorption data.

The Freundlich equation, an empirical adsorption model, is written as (Mahmoud et al. 2017):

$$\log Q_e = \log K_F + \frac{1}{n}\log C_e \tag{13}$$

where C_e and Q_e are defined earlier, K_F is the Freundlich constant ($\text{mmol}^{1-n}\ \text{L}^n/\text{g}$), and n is a measure of the heterogeneity of adsorption sites on the adsorbent surface (Essington 2004). If $1/n$ approaches 0, the surface site heterogeneity increases and there is a broad distribution of adsorption site types. On the other hand, if $1/n$ approaches unity, the surface site homogeneity increases and there is a narrow distribution of adsorption site types. This model can describe the adsorption data if the plot of $\log Q_e$ against $\log C_e$ gives a straight line with slope $1/n$ and a Y-intercept of $\log K_F$.

The Temkin isotherm model supposes that the adsorbate-adsorbate repulsions causes the heat of adsorption of all species to decrease linearly, instead of logarithmically as the Freundlich model, with coverage and its linear form is presented by the following equation (Temkin and Pyzhev 1940):

$$Q_e = B\ln A + B\ln C_e \tag{14}$$

where B is related to the heat of adsorption (J/mol) and A is the Temkin isotherm constant corresponding to the maximum binding energy (L/g). For the validity of this model, the plot of $\ln C_e$ versus Q_e should give a linear plot with slope of B and a Y-intercept of $B \ln A$.

The linear form of the generalized isotherm model, which is a combination of Langmuir and Freundlich isotherms, is given by (Gupta and Babu 2009):

$$\log\left(\frac{Q_m}{Q_e} - 1\right) = \log K_G - N\log C_e \tag{15}$$

where K_G and N are the generalized isotherm constants and are obtained from the intercept and slope of the linear plot of $\log [(Q_m/Q_e) - 1]$ versus $\log C_e$. In this equation, Q_m is obtained from Langmuir isotherm model.

Figure 9 a–d shows the plots of Langmuir, Freundlich, Temkin, and generalized isotherm models at different temperatures, respectively. The calculated parameters of these models as well as the correlation coefficient (R^2) values are also presented in this figure (Table 1). By comparing the R^2 values obtained for the abovementioned isotherm models at the studied temperatures, it can be seen that fitting the present equilibrium data to Langmuir and Freundlich equations resulted in linear plots with higher R^2 values (R^2 ranging from 0.975 to 0.996) than those obtained for Temkin ($R^2 = 0.917$–0.954) and generalized ($R^2 = 0.797$–0.879) models. This finding implies that both Langmuir and Freundlich isotherm models had the ability to well describe the equilibrium data of cobalt(II) radionuclides onto the modified montmorillonite. From Fig. 9 b, the calculated values of $1/n$ are found to be much closer to 0 than to unity, indicating that the surface heterogeneity increased and there is a broad distribution of adsorption site types. On the other hand, the calculated values of Q_m obtained for the Langmuir isotherm model (Fig. 9a; Table 1) increased from 0.591 to 0.796 mmol/g as the temperature is increased from 30 to 60 °C. These data pointed out that the present adsorption process is endothermic in nature. One of the fundamental characteristics of Langmuir isotherm is a dimensionless constant called separation factor, R_L, which is defined by:

$$R_L = \frac{1}{1 + K_L C_o} \tag{16}$$

The values of R_L are used to predict whether the adsorption process is favorable ($0 < R_L < 1$), unfavorable ($R_L > 1$), linear

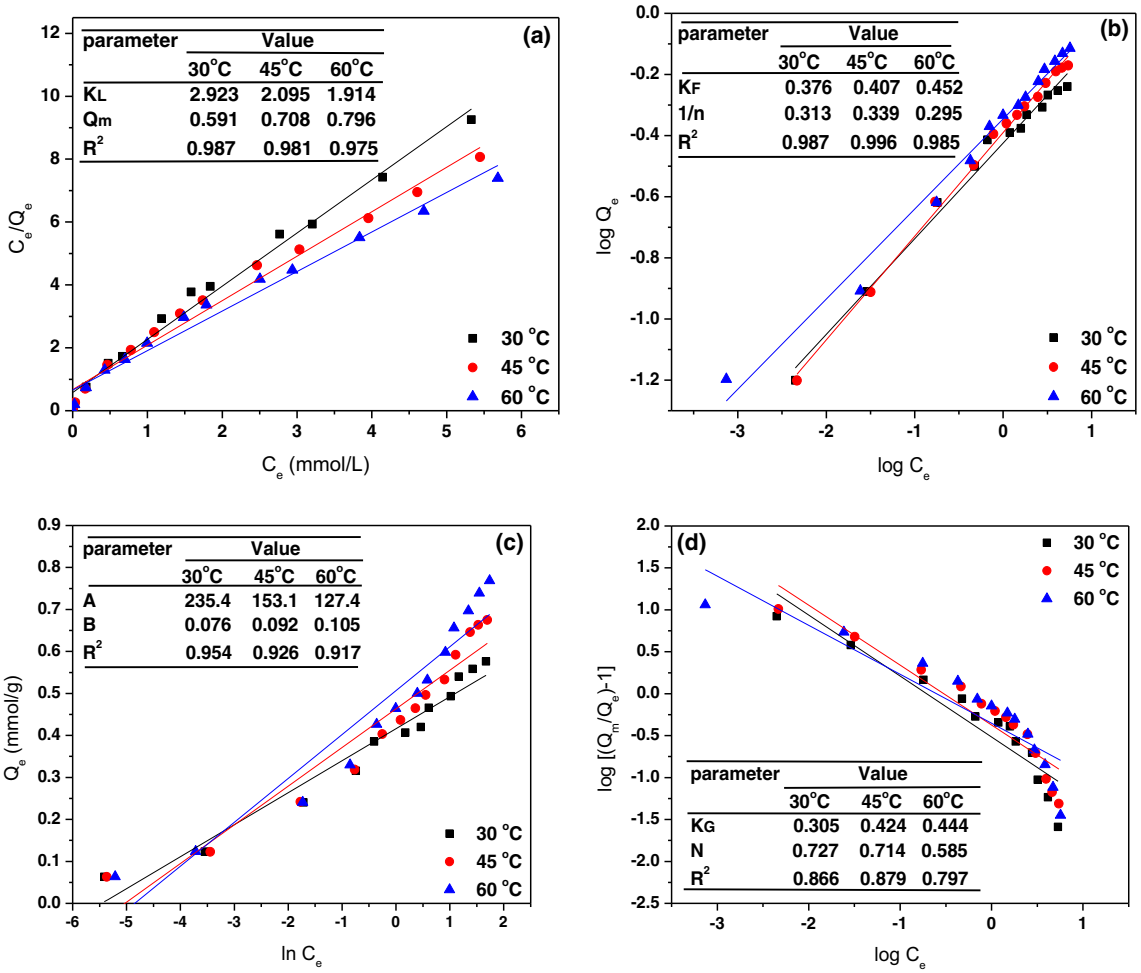

Fig. 9 Linear fittings of the equilibrium isotherms of cobalt(II) radionuclides onto TMM to Langmuir (**a**), Freundlich (**b**), Temkin (**c**), and generalized (**d**) isotherm models

($R_L = 1$), or irreversible ($R_L = 0$). The calculated values of R_L at the studied initial cobalt(II) concentrations are found to be in the ranges of 0.461–0.047, 0.509–0.065, and 0.507–0.071 at temperatures of 30, 45, and 60 °C, revealing the favorability of the present adsorption process.

Based on the K_L values obtained at different temperatures for the Langmuir model, the thermodynamic parameters (enthalpy change, ΔH°, and entropy change, ΔS°) are calculated from the slope and intercept of the linear plot of ln K_L versus $1/T$ according to the following relation (Ghassabzadeh et al. 2010):

$$\ln K_L = -\frac{\Delta H^o}{RT} + \frac{\Delta S^o}{R} \tag{17}$$

where R is the universal gas constant ($R = 0.008314$ kJ/mol) and T is the absolute temperature in degree Kelvin. Afterwards, values of the change in free energy (ΔG°) are calculated based on the values of ΔH° and ΔS° (ΔG° = ΔH−TΔS°).

The calculated values of ΔG° are found to be − 2.687, − 3.407, and − 4.127 kJ/mol at temperatures of 30, 45, and 60 °C, respectively. The minus sign of ΔG° values indicates that adsorption of cobalt(II) radionuclides onto the modified montmorillonite is a spontaneous process. By shedding more light on these values, it can be observed that ΔG° is more negative at high temperature, indicating the increase of the adsorption spontaneity with increasing temperature. Furthermore, the value of ΔG° can be generally used to distinguish between physical and chemical adsorption processes. If ΔG° ranges between 0 and − 20 kJ/mol, the adsorbate is physically adsorbed onto the solid phase, while it is chemically adsorbed if ΔG° ranges between − 80 and − 400 kJ/mol (Petrucci and Harwood 1997). From the aforementioned ΔG° values, it can be deduced that removal of cobalt(II) radionuclides onto TMM is governed by physical adsorption mechanism. The positive value of the enthalpy change (ΔH° = 11.857 kJ/mol) suggested that adsorption of cobalt(II) radionuclides onto the modified montmorillonite is endothermic process and heat is gained from the surroundings.

This low value of ΔH° further indicates that cobalt(II) radionuclides are removed via physical adsorption. Eventually, the positive value of the entropy change (ΔS° = 0.048 kJ/mol K) illustrates that the degree of randomness at the solid-solution interface increased during the adsorption process.

Comparison with natural, organo-modified, and inorgano-modified clays

To show the significance of the proposed modification process in the current investigation, the maximum adsorption capacity of cobalt(II) achieved by TH-modified montmorillonite (Q_{max} = 0.85 mmol/g ≈ 50.09 mg/g) is compared with those reported in literature for various metal ions using natural, organo-modified, and inorgano-modified clays. These values are tabulated in Table 1. This table demonstrates that TH-modified montmorillonite is obviously exhibited higher adsorption capacity not only than the natural clays, but also than the modified ones and hence its potentiality for remediation of radioactive liquid wastes.

Desorption studies

Figure 10 illustrates the influence of desorbing agent concentrations (0.001–0.1 mol/L) on the desorption percentage of cobalt(II)-loaded organo-montmorillonite. Except for Al^{3+}, the data presented in this figure show that the desorbing agent concentration played a significant role in the desorption process of cobalt(II)-loaded TMM. Increasing the desorbing agent concentration, either organic or inorganic, concentration resulted in an increase in the desorption percentage of cobalt(II) radionuclides and maximum desorption percentage of about 90% is achieved by Al^{3+} and EDTA at concentrations ≥ 0.01 mol/L. This high desorption percentage proposed that most of cobalt(II) radionuclides are adsorbed onto the active sites of the modifying agent, TH, as well as the external adsorption sites of montmorillonite. While the fraction remained onto TMM, 10% of adsorbate could not be desorbed, clarified that insignificant amount of cobalt(II) radionuclides are adsorbed onto the internal adsorption sites of montmorillonite. From the desorption data (Fig. 10), it can be eventually concluded that cobalt(II) radionuclides are physically adsorbed onto TH-modified montmorillonite.

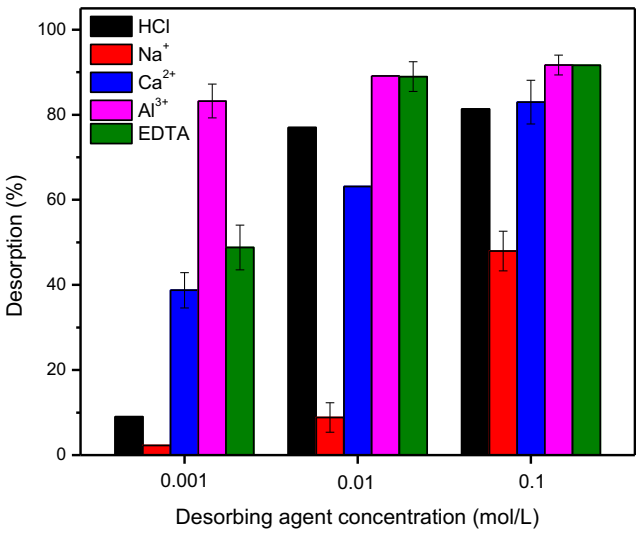

Fig. 10 Desorption of cobalt(II) radionuclides loaded onto TMM using various desorbing agents

Conclusions

TMM was efficiently applied as an adsorbent for cobalt(II) radionuclides from aqueous solutions. From the data obtained, it can be inferred that

i. The removal efficiency of cobalt(II) radionuclides was strongly dependent on the amount of modifying agent loaded onto montmorillonite as well as the loading pH. Modification of montmorillonite was confirmed by FTIR, while the XRD results showed that TH was bound to the clay at the external adsorption sites rather than the interlayer space.
ii. Removal percentage > 99% was attained for cobalt(II) radionuclides in the pH range of 3.5–7 using TMM compared to 63% at pH ≥ 5.4 using the unmodified clay.
iii. Increasing the adsorbent dosage of TMM from 2 g/L (*V*/*M* = 0.5 L/g) to 20 g/L (*V*/*M* = 0.05 L/g) increased the removal percentage of Co(II) from 21.5 to 99.2%, while decreased the amount adsorbed from 0.199 mmol/g to 0.084 mmol/L.
iv. Kinetic studies revealed that maximum removal percentages of 41.2%, 69.9%, and 99.7% were achieved for 0.4, 0.2, and 0.1 mmol/L cobalt(II) at equilibrium times of 30, 20, and 10 min, respectively. Modeling of the kinetic data demonstrated that the pseudo-second order model was the best one for describing the present adsorption process. The diffusion study suggested that the present adsorption process was controlled by film diffusion.
v. Ionic strength had no effect on the removal percentage of cobalt(II) up to 0.001 M. Beyond this value, the removal percentage decreased to about 40% at 0.1 M NaCl.
vi. Equilibrium isotherms show that increasing temperature from 30 to 60 °C increased the adsorption capacity from 0.576 to 0.769 mmol/g. Both Langmuir and Freundlich isotherm models had the ability to represent the equilibrium isotherms data.
vii. Thermodynamic parameters inferred that cobalt(II) radionuclides were physically adsorbed onto TMM (ΔG° = − 2.687, − 3.407 and − 4.127 kJ/mol at temperatures of 30, 45, and 60 °C, respectively) and it was an endothermic in nature (ΔH° = 11.857 kJ/mol).

viii. The adsorption capacity of TMM was higher than those reported for natural, organo-modified, and inorgano-modified clays and consequently it has the potentiality to be used as an adsorbent for removal of cobalt(II) radionuclides from radioactive liquid wastes.

References

Abdul Nishad P, Bhaskarapillai A, Velmurugan S, Narasimhan SV (2012) Cobalt (II) imprinted chitosan for selective removal of cobalt during nuclear reactor decontamination. Carbohydr Polym 87:2690–2696. https://doi.org/10.1016/j.carbpol.2011.11.061

Bhattacharyya KG, Gupta SS (2006) Kaolinite, montmorillonite, and their modified derivatives as adsorbents for removal of Cu(II) from aqueous solution. Sep Purif Technol 50:388–397. https://doi.org/10.1016/j.seppur.2005.12.014

Boyd GE, Adamson AW, Myers LS (1947) The exchange adsorption of ions from aqueous solutions by organic zeolites: II. Kinetics. J Am Chem Soc 69:2836–2848 https://pubs.acs.org/doi/10.1021/ja01203a066

Chen CL, Wang XK (2007) Sorption of Th (IV) to silica as a function of pH, humic/fulvic acid, ionic strength, electrolyte type. Appl Radiat Isot 65:155–163. https://doi.org/10.1016/j.apradiso.2006.07.003

Chen L, Yu S, Liu B, Zuo L (2012) Removal of radiocobalt from aqueous solution by different sized carbon nanotubes. J Radioanal Nucl Chem 292:785–791. https://doi.org/10.1007/s10967-011-1514-z

Combernoux N, Schrive L, Labed V, Wyart Y, Carretier E, Moulin P (2017) Treatment of radioactive liquid effluents by reverse osmosis membranes: from lab-scale to pilot-scale. Water Res 123:311–320. https://doi.org/10.1016/j.watres.2017.06.062

Derakhshani E, Naghizadeh A (2018) Optimization of humic acid removal by adsorption onto bentonite and montmorillonite nanoparticles. J Mol Liq 259:76–81. https://doi.org/10.1016/j.molliq.2018.03.014

Długosz O, Banach M (2018) Kinetic, isotherm and thermodynamic investigations of the adsorption of Ag^{+} and Cu^{2+} on vermiculite. J Mol Liq 258:295–309. https://doi.org/10.1016/j.molliq.2018.03.041

Essington ME (2004) Soil and water chemistry: an integrative approach. CRC Press LLC, Boca Raton

Ezzat A, Mahmoud MR, Soliman MA, Saad EA, Kandeel A (2017) Evaluation of sorptive flotation technique for enhanced removal of radioactive Eu(III) from aqueous solutions. Radiochim Acta 105:205–213. https://doi.org/10.1515/ract-2016-2618

Ferhat M, Kadouche S, Drouiche N, Messaoudi K, Messaoudi B, Lounici H (2016) Competitive adsorption of toxic metals on bentonite and use of chitosan as flocculent coagulant to speed up the settling of generated clay suspensions. Chemosphere 165:87–93. https://doi.org/10.1016/j.chemosphere.2016.08.125

Gao Y, Shao Z, Xiao Z (2015) U(VI) sorption on illite: effect of pH, ionic strength, humic acid and temperature. J Radioanal Nucl Chem 303:867–876. https://doi.org/10.1007/s10967-014-3385-6

Ghassabzadeh H, Torab-Mostaedi M, Mohaddespour A, Maragheh MG, Ahmadi SJ, Zaheri P (2010) Characterizations of Co(II) and Pb(II) removal process from aqueous solutions using expanded perlite. Desalination 261:73–79. https://doi.org/10.1016/j.desal.2010.05.028

Giles CH, McEvan TH, Nakhwa SN, Smith D (1960) Studies in adsorption: part XI. A system of classification of solution adsorption isotherms, and its use in diagnosis of adsorption mechanisms and in measurement of specific surface areas of solids. J Chem Soc 4:3973–3993. https://doi.org/10.1039/jr9600003973

Gok O, Ozcan A, Erdem B, Ozcan AS (2008) Prediction of the kinetics, equilibrium and thermodynamic parameters of adsorption of copper(II) ions onto 8-hydroxy quinolone immobilized bentonite. Colloids Surf A Physicochem Eng Asp 317:174–185. https://doi.org/10.1016/j.colsurfa.2007.10.009

Gu P, Zhang S, Li X, Wang X, Wen T, Jehan R, Alsaedi A, Hayat T, Wang X (2018) Recent advances in layered double hydroxide-based nanomaterials for the removal of radionuclides from aqueous solution. Environ Pollut 240:493–505. https://doi.org/10.1016/j.envpol.2018.04.136

Guerra DJL, Mello I, Resende R, Silva R (2013) Application as absorbents of natural and functionalized Brazilian bentonite in Pb^{2+} adsorption: equilibrium, kinetic, pH, and thermodynamic effects. Water Resour Industry 4:32–50. https://doi.org/10.1016/j.wri.2013.11.001

Guo Z, Li Y, Zhang S, Niu H, Chen Z, Xu J (2011) Enhanced sorption of radiocobalt from water by Bi(III) modified montmorillonite: a novel adsorbent. J Hazard Mater 192:168–175. https://doi.org/10.1016/j.jhazmat.2011.05.004

Gupta S, Babu BV (2009) Removal of toxic metal Cr(VI) from aqueous solutions using sawdust as adsorbent: equilibrium, kinetics and regeneration studies. Chem Eng J 150:352–365. https://doi.org/10.1016/j.cej.2009.01.013

Han H, Cheng C, Hu S (2017) Facile synthesis of gelatin modified attapulgite for the uptake of uranium from aqueous solution. J Mol Liq 234:172–178. https://doi.org/10.1016/j.molliq.2017.03.076

He M, Zhu Y, Yang Y, Han B, Zhang Y (2011) Adsorption of cobalt(II) ions from aqueous solutions by palygorskite. Appl Clay Sci 54:292–296. https://doi.org/10.1016/j.clay.2011.09.013

Ho YS, McKay G (1999) Pseudo-second order model for sorption process. Process Biochem 34:451–465. https://doi.org/10.1016/S0032-9592(98)00112-5

IAEA (1981) Decontamination of operational nuclear power plants, Vienna, IAEATECDOC-248. https://inis.iaea.org/collection/NCLCollectionStore/_Public/13/680/13680247.pdf

Jiang M, Jin X, Lu X, Chen Z (2010) Adsorption of Pb(II), cd(II), Ni(II) and cu(II) onto natural kaolinite clay. Desalination 252(2010):33–39. https://doi.org/10.1016/j.desal.2009.11.005

Kebabi B, Terchi S, Bougherara H, Reinert L, Duclaux L (2017) Removal of manganese (II) by edge site adsorption on raw and milled vermiculites. Appl Clay Sci 139:92–98. https://doi.org/10.1016/j.clay.2016.12.041

Lagergren S (1898) About the theory of so-called adsorption of soluble substances. Kungl Svenska vetenskapsakademiens handlingar 241:1–39

Langmuir L (1918) Adsorption of gases on plane surfaces of glass, mica and platinum. J Am Chem Soc 40:1361–1403. https://doi.org/10.1021/ja02242a004

Lazarevic S, Jankovic-Castvan I, Potkonjak B, Janackovic D, Petrovic R (2012) Removal of Co^{2+} ions from aqueous solutions using iron-functionalized sepiolite. Chem Eng Process 55:40–47. https://doi.org/10.1016/j.cep.2012.01.004

Liu X, Cheng C, Xiao C, Shao D, Xu Z, Wang J, Hu S, Li X, Wang W (2017) Polyaniline (PANI) modified bentonite by plasma technique for U(VI) removal from aqueous solution. Appl Surf Sci 411:331–337. https://doi.org/10.1016/j.apsusc.2017.03.095

Mahmoud MR, Othman SH (2018) Efficient decontamination of naturally occurring radionuclide from aqueous carbonate solutions by ion flotation process. Radiochim Acta 106:465–476

Mahmoud MR, Sharaf El-deen G, Soliman MA (2014) Surfactant-impregnated activated carbon for enhanced adsorptive removal of Ce(IV) radionuclides from aqueous solutions. Ann Nucl Energy 72:134–144. https://doi.org/10.1016/j.anucene.2014.05.006

Mahmoud MR, Soliman MA, Allan KF (2015) Adsorption behavior of samarium(III) from aqueous solutions onto PAN@SDS core-shell polymeric adsorbent. Radiochim Acta 103:443–456. https://doi.org/10.1515/ract-2014-2299

Mahmoud MR, Rashad GM, Metwally E, Saad EA, Elewa AM (2017) Adsorptive removal of $^{134}Cs^{+}$, $^{60}Co^{2+}$ and $^{152+154}Eu^{3+}$ radionuclides from aqueous solutions using sepiolite: single and multi-component systems. Appl Clay Sci 141:72–80. https://doi.org/10.1016/j.clay.2016.12.021

Manohar DM, Noeline BF, Anirudhan TS (2006) Adsorption performance of Al-pillared bentonite clay for the removal of cobalt(II) from aqueous phase. Appl Clay Sci 31:194–206. https://doi.org/10.1016/j.clay.2005.08.008

Marco-Brown JL, Guz L, Olivelli MS, Schampera B, Sánchez RMT, Curutchet G, Candal R (2018) New insights on crystal violet dye adsorption on montmorillonite: kinetics and surface complexes studies. Chem Eng J 333:495–504. https://doi.org/10.1016/j.cej.2017.09.172

Margerum DW, Byrd SH, Reed SA, Banks CV (1953) Preparation and properties of 2-(2-Hydroxy-3,6-disulfo-1-naphthylazo)-benzenearsonic acid (Thorin). Anal Chem 25:1219–1221 https://pubs.acs.org/doi/abs/10.1021/ac60080a022

Metwally SS, Ayoub RR (2016) Modification of natural bentonite using a chelating agent for sorption of ^{60}Co radionuclide from aqueous solution. Appl Clay Sci 126:33–40. https://doi.org/10.1016/j.clay.2016.02.021

Mukhopadhyay R, Manjaiah KM, Datta SC, Yadav RK, Sarkar B (2017) Inorganically modified clay minerals: preparation, characterization, and arsenic adsorption in contaminated water and soil. Appl Clay Sci 147:1–10. https://doi.org/10.1016/j.clay.2017.07.017

Omar H, Arida H, Daifullah A (2009) Adsorption of ^{60}Co radionuclides from aqueous solution by raw and modified bentonite. Appl Clay Sci 44(2009):21–26. https://doi.org/10.1016/j.clay.2008.12.013

Osmanlioglu AE (2018) Decontamination of radioactive wastewater by two-staged chemical precipitation. Nucl Eng Technol 50:886–889. https://doi.org/10.1016/j.net.2018.04.009

Petrucci RH, Harwood WS (1997) General chemistry: principles and modern applications, 7th ed. Prentice Hall, New Jersey

Rashad GM, Mahmoud MR, Elewa AM, Metwally E, Ebtissam AS (2016) Removal of radiocobalt from aqueous solutions by adsorption onto low-cost adsorbents. J Radioanal Nucl Chem 309:1065–1076. https://doi.org/10.1007/s10967-016-4726-4

Rashad GM, Soliman M, Mahmoud MR (2018) Removal of radioselenium oxyanions from aqueous solutions by adsorption onto hydrous zirconium oxide. J Radioanal Nucl Chem 317:593–603. https://doi.org/10.1007/s10967-018-5916-z

Rathnayake SI, Martens WN, Xi Y, Frost RL, Ayoko GA (2017) Remediation of Cr (VI) by inorganic-organic clay. J Colloid Interface Sci 490:163–173. https://doi.org/10.1016/j.jcis.2016.11.070

Ren X, Zhang Z, Luo H, Hu B, Dang Z, Yang C, Li L (2014) Adsorption of arsenic on modified montmorillonite. Appl Clay Sci 97–98:17–23. https://doi.org/10.1016/j.clay.2014.05.028

Shahwan T, Erten HN, Unugur S (2006) A characterization study of some aspects of the adsorption of aqueous Co^{2+} ions on a natural bentonite clay. J Colloid Interface Sci 300:447–452. https://doi.org/10.1016/j.jcis.2006.04.069

Sparks DL (2003) Environmental soil chemistry, second edition. Academic Press, Elsevier Science, USA

Temkin MJ, Pyzhev V (1940) Kinetics of ammonia synthesis on promoted iron catalysts. Acta Physiochim URSS 12:327–356

Unuabonah EI, Adebowale KO, Olu-Owolabi BI, Yang LZ, Kong LX (2008) Adsorption of Pb(II) and Cd (II) from aqueous solutions onto sodium tetraborate-modified kaolinite clay: equilibrium and thermodynamic studies. Hydrometallurgy 93:1–9. https://doi.org/10.1016/j.hydromet.2008.02.009

Wang G, Hua Y, Su X, Komarneni S, Ma S, Wang Y (2016) Cr(VI) adsorption by montmorillonite nanocomposites. Appl Clay Sci 124–125:111–118. https://doi.org/10.1016/j.clay.2016.02.008

Wang J, Chen Z, Shao D, Li Y, Xu Z, Cheng C, Asiri AM, Marwani HM, Hu S (2017) Adsorption of U(VI) on bentonite in simulation environmental conditions. J Mol Liq 242:678–684. https://doi.org/10.1016/j.molliq.2017.07.048

Weber WJ, Morris JC (1963) Kinetics of adsorption on carbon from solution. J Sanit Eng Div 89:31–60

Xiao Y, Huang L, Long Z, Feng Z, Wang L (2016) Adsorption ability of rare earth elements on clay minerals and its practical performance. J Rare Earths 34:543–548. https://doi.org/10.1016/S1002-0721(16)60060-1

Yao W, Yu S, Wang J, Zou Y, Lu S, Ai Y, Alharbi SN, Alsaedi A, Hayat T, Wang X (2017) Enhanced removal of methyl orange on calcined glycerol-modified nanocrystallined Mg/Al layered double hydroxides. Chem Eng J 307:476–486. https://doi.org/10.1016/j.cej.2016.08.117

Yusan S, Gok C, Erenturk S, Aytas S (2012) Adsorptive removal of thorium (IV) using calcined and flux calcined diatomite from Turkey: evaluation of equilibrium, kinetic and thermodynamic data. Appl Clay Sci 67–68:106–116. https://doi.org/10.1016/j.clay.2012.05.012

Zhu H, Xiao X, Guo Z, Han X, Liang Y, Zhang Y, Zhou C (2018) Adsorption of vanadium (V) on natural kaolinite and montmorillonite: characteristics and mechanism. Appl Clay Sci 161:310–316. https://doi.org/10.1016/j.clay.2018.04.035